



HAL
open science

Persistent homology reveals strong phylogenetic signal in 3D protein structures

Léa Bou Dagher, Dominique Madern, Philippe Malbos, Céline
Brochier-Armanet

► **To cite this version:**

Léa Bou Dagher, Dominique Madern, Philippe Malbos, Céline Brochier-Armanet. Persistent homology reveals strong phylogenetic signal in 3D protein structures. PNAS Nexus, 2024, 3 (4), pp.158. 10.1093/pnasnexus/pgae158 . hal-04599673

HAL Id: hal-04599673

<https://hal.science/hal-04599673>

Submitted on 3 Jun 2024

HAL is a multi-disciplinary open access archive for the deposit and dissemination of scientific research documents, whether they are published or not. The documents may come from teaching and research institutions in France or abroad, or from public or private research centers.

L'archive ouverte pluridisciplinaire **HAL**, est destinée au dépôt et à la diffusion de documents scientifiques de niveau recherche, publiés ou non, émanant des établissements d'enseignement et de recherche français ou étrangers, des laboratoires publics ou privés.



Distributed under a Creative Commons Attribution 4.0 International License

Persistent homology reveals strong phylogenetic signal in 3D protein structures

Léa Bou Dagher ^{a,b,c}, Dominique Madern ^d, Philippe Malbos ^{b,*} and Céline Brochier-Armanet ^{a,*}

^aUniversité Claude Bernard Lyon 1, CNRS, VetAgro Sup, Laboratoire de Biométrie et BiologieÉvolutive, UMR5558, F-69622 Villeurbanne, France

^bUniversité Claude Bernard Lyon 1, CNRS, Institut Camille Jordan, UMR5208, F-69622 Villeurbanne, France

^cUniversité Libanaise, Laboratoire de Mathématiques, École Doctorale en Science et Technologie, PO BOX 5 Hadath, Liban

^dUniversity Grenoble Alpes, CEA, CNRS, IBS, 38000 Grenoble, France

*To whom correspondence should be addressed: Email: celine.brochier-armanet@univ-lyon1.fr, philippe.malbos@univ-lyon1.fr

Edited By: Gerhard Hummer

Abstract

Changes that occur in proteins over time provide a phylogenetic signal that can be used to decipher their evolutionary history and the relationships between organisms. Sequence comparison is the most common way to access this phylogenetic signal, while those based on 3D structure comparisons are still in their infancy. In this study, we propose an effective approach based on Persistent Homology Theory (PH) to extract the phylogenetic information contained in protein structures. PH provides efficient and robust algorithms for extracting and comparing geometric features from noisy datasets at different spatial resolutions. PH has a growing number of applications in the life sciences, including the study of proteins (e.g. classification, folding). However, it has never been used to study the phylogenetic signal they may contain. Here, using 518 protein families, representing 22,940 protein sequences and structures, from 10 major taxonomic groups, we show that distances calculated with PH from protein structures correlate strongly with phylogenetic distances calculated from protein sequences, at both small and large evolutionary scales. We test several methods for calculating PH distances and propose some refinements to improve their relevance for addressing evolutionary questions. This work opens up new perspectives in evolutionary biology by proposing an efficient way to access the phylogenetic signal contained in protein structures, as well as future developments of topological analysis in the life sciences.

Keywords: topological data analysis, phylogenetics, persistent homology, protein 3D structure

Significance Statement

Determining the extent to which the 3D structures of proteins contain a phylogenetic signal is both a challenge and a major issue in evolutionary biology. Access to this information is key to studying very ancient evolutionary events, as protein structures are thought to evolve more slowly than sequences. However, the lack of reliable and efficient methods limits the use of structures. Here we propose an original approach based on persistent homology, an algorithmic method of topological data analysis. Analysis of 22,940 sequences and structures representing 763,648 homologous protein pairs shows that structures contain a strong phylogenetic signal that is efficiently captured by this approach, paving the way for the use of structures to study protein evolution.

Introduction

Proteins are composed of one or more linear chains of amino acids, whose 3D fold (hereafter referred to as structure) is determined by the order and the physicochemical properties of the amino acids. In addition to their essential role in cells, proteins carry a phylogenetic (i.e. historical) signal. During evolution, amino acid substitutions, insertions, and deletions occur in protein sequences, which can affect their structure and function. These changes are transmitted over time vertically from parent to offspring or horizontally by gene transfer between unrelated organisms. Analyzing changes in protein sequences therefore provides information about the protein evolutionary history and the relationships between organisms. Phylogenetic inference by sequence

comparison is the classic way to analyze the historical signal contained in protein sequences. Although very effective, this approach has some limitations (1–3). In particular, it is known that amino acids interact tightly, both functionally and spatially within protein structures, affecting their evolutionary trajectories. However, to reduce algorithmic complexity, the simplifying assumption that amino acids are independent of each other is often made, even though taking this information into account could improve the accuracy of evolutionary models, sequence alignments, and thus phylogenetic inference (4–8). In addition, most evolutionary models only consider substitutions and ignore the signal carried by insertions and deletions (indels), which could lead to an underestimation of the true evolutionary divergence between sequences (9, 10). Finally, the construction of reliable multiple

Competing Interest: The authors declare no competing interest.

Received: November 2, 2023. **Accepted:** April 1, 2024

© The Author(s) 2024. Published by Oxford University Press on behalf of National Academy of Sciences. This is an Open Access article distributed under the terms of the Creative Commons Attribution License (<https://creativecommons.org/licenses/by/4.0/>), which permits unrestricted reuse, distribution, and reproduction in any medium, provided the original work is properly cited.

alignments and phylogenetic trees is challenging, especially when sequences are highly divergent, because multiple substitutions (i.e. the occurrence of more than one substitution at a given amino acid site over time) lead to the progressive erosion of the phylogenetic signal (3, 11).

In this context, the analysis of protein structures has been proposed as an interesting alternative, as they are assumed to evolve more slowly than protein sequences (12). In fact, homologous proteins could share the same fold and other structural features even when their sequences have diverged beyond recognition (13–16). Furthermore, studying structures allows the spatial proximity of amino acids and their interactions to be considered. However, the use of structures to address evolutionary questions is still in its infancy due to the limited number of structures available in databases and methodological issues such as the lack of models accounting for structural evolution (see (17, 18) and references therein). The recent development of efficient structure prediction methods, such as AlphaFold2 (19), has removed the first barrier by providing virtually unlimited access to structural information (20, 21). Methodologically, most studies are based on pairwise comparisons of structures, either by direct comparison of structures via structural alignment, or by comparison of vectors encoding their structural features (e.g. secondary structures, local features, atom density) (22–37). In most cases only the C α atoms of the protein backbone are considered; the other atoms being ignored. These scores are then converted into distances and used to construct phylogenetic trees (38). However, as with protein sequence alignment, structural alignment is often difficult. The main consequence is that different alignments can be obtained depending on the algorithms used (16, 39). Alternative approaches to build phylogenies from structures are based on the taxonomic distribution of protein folds. Specifically, the presence or the absence of known folds in the organisms under study is encoded in a character matrix, which is then used to reconstruct phylogenetic trees by maximum parsimony or maximum likelihood methods (40–42).

In this work, we explore the potential of persistent homology (PH) to capture the phylogenetic signal from protein structures. PH is one of the most notable topological data analysis method (43) and a rapidly growing area of research with applications in a wide range of fields, including life sciences and biomedicine (44–51). PH provides robust and efficient algorithms for geometrically characterizing datasets represented by noisy finite point clouds (PCs). PH algorithms track the topological features (e.g. connected components, cycles, cavities, tunnels) of a given PC at different spatial scales. The principle is to examine the persistence of these features through multiscale filtration, turning the PC into a combinatorial object describing topological feature changes at increasing scales. This filtration thus captures the main and most robust topological features within the PC amidst the noise. These features are described by combinatorial signatures called PH-descriptors (e.g. barcodes, persistence landscapes), which represent the topological signatures of the PCs. For more details on PH see the [Supplementary Material](#) text and Figs. S1–S7. The stability properties of PH ensure its robustness to noise by indicating how stable the information retained in the PH-descriptors is under small variations in the data (52) (see also [Supplementary Material](#) text). PCs can be compared by computing distances (hereafter referred to as PH-distances) between their PH-descriptors, of which the most used are the Bottleneck (Btk), Wasserstein (Ws), and Landscape (Ls) distances (see [Supplementary Material](#) text). PH is therefore particularly well suited to analyzing and comparing protein structures, which

can be represented by noisy 3D PCs, whose points represent the spatial coordinates of the amino acid atoms. The noise in PCs can be due to, for example, the experimental precision with which structures are resolved, the uncertainty of bioinformatic predictions, or natural slight variations in protein shape. To date, PH has been mainly used to study protein folding, to classify protein structures, for protein engineering and directed protein evolution, and to study the effect of mutations on protein binding (53–61), but it has never been used to study the phylogenetic signal that may be contained in protein structures.

In this study, we performed a large-scale analysis of 518 protein families, comprising 22,940 protein sequences and structures, from 10 major prokaryotic groups. By comparing the corresponding 763,648 pairs of homologous proteins, we show that PH captures a strong signal in protein structures and that this signal is predominantly phylogenetic. This suggests that PH is an efficient way to extract phylogenetic information from protein structures and opens up a promising new area of application for PH in the life sciences.

Results

Reliability of predicted protein structures AlphaFold2

The reliability of structure predictions for the 22,940 proteins considered was assessed by comparing the predictions of AlphaFold2 with experimentally resolved structures from the RCSB PDB. All root-mean-square deviation (RMSD) values are between 0.05 to 3.53 Å (Fig. S8). In addition, 94% of the C α have a confidence index (CI) greater than or equal to 70%, and 83% greater than or equal to 90%. Furthermore, 99% of the predicted structures have an average C α CI greater than or equal to 70%, and 80% greater than or equal to 90% (Figs. S9 and S10). Overall, this suggests that protein structures predicted by AlphaFold2 are reliable and can be used for further investigation.

Persistent homology distances computation

For each of the 763,648 pairs of homologous proteins, we calculated PH-distances (i.e. Btk-distances, Ws-distances, and Ls-distances) in homological dimension 1 and 2 by applying alpha complex (AC) and Vietoris-Rips (VR) filtrations to the corresponding structures. Here, PCs corresponding to C α atoms (PC(C α)) were used, as they are assumed to be representative of the whole structure and require less computation time than considering all atoms (55). At this stage, we find strong and significant correlations between PH-distances and the number of points in PC(C α) ($r = 0.39$ – 0.61 , all P -values $< 3.8 \times 10^{-3}$, Fig. 1A and B and Table S1). This means that the number of C α contained in structures has a significant impact on PH-distances. In order to limit this effect, we normalized PH-distances by the average number of C α of the two compared PCs (Figs. S11 and S12). This normalization appears to be efficient because previously observed correlations become nonsignificant ($r = -0.11$ – -5×10^{-4} , all P -values > 0.1 , Fig. 1C and D and Table S1). Accordingly, we used normalized PH-distances in all analyses.

Since the shape of proteins is constrained by various physicochemical considerations, such as covalent or hydrogen bonds, we investigated whether the PH-distances calculated between pairs of homologous protein structures contained any biological information or whether they could have been observed by chance alone. We therefore compared the ranges of Btk-distances,

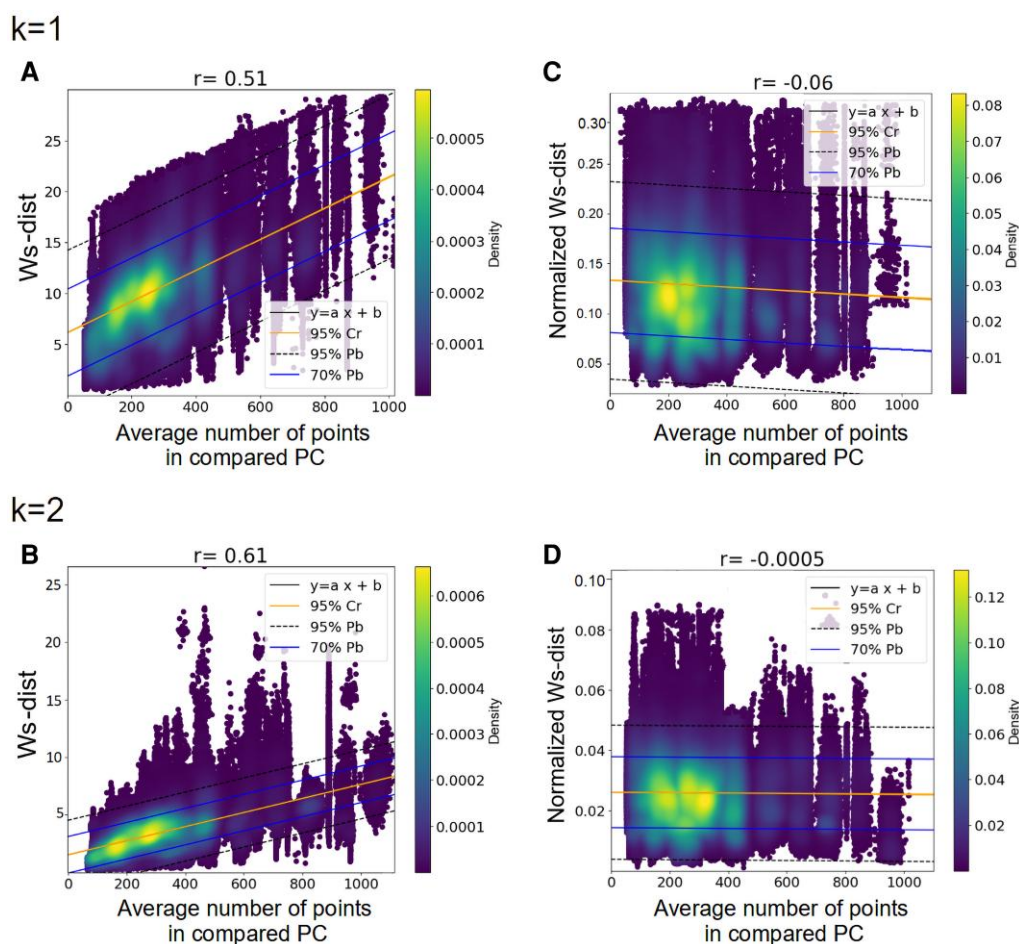


Fig. 1. Correlation plots between the average number of points in PC(C α) and Ws-distances calculated by AC filtration on PC(C α) of the AlphaFold2 predictions. Each plot contains 763,648 points, each corresponding to one pair of homologous proteins for which the average number of points of the two PC(C α) (x-axis) is compared with the Ws-distance (y-axis). Results obtained with other PH-distances are shown as Table S1. A) Ws-distances ($k=1$), $r=0.51$, P -value = 2×10^{-5} , B) Ws-distances ($k=2$), $r=0.61$, P -value = 1.7×10^{-5} , C) Normalized Ws-distances ($k=1$), $r=-0.06$, P -value = 0.1, D) normalized Ws-distances ($k=2$), $r=-0.0005$, P -value = 0.2. For each panel, the central line is the 95% confidence regions in which the true regression line should belong. The two intermediate lines are the 70% interval within which future individual data points or observations should fall. The two most external lines are the 95% interval within which a future individual data point or observation should fall. The black line corresponds to the regression line ($y = ax + b$). Point colors correspond to the density values according to the density scale.

Ws-distances, and Ls-distances calculated between randomly selected 7,500 pairs of homologous protein structures and 7,500 pairs of nonhomologous protein structures. We find that the latter are significantly larger than the former, in both homological dimensions 1 and 2 (Fig. S13). This means that the PH-distances calculated from homologous proteins cannot have been obtained by chance and contain biological information.

We also observe that the normalized Ls-distances and Ws-distances are close to each other, but larger than the Btk-distances (Figs. S11 and S12). This difference is expected because the Btk-distance corresponds to the largest distance between pairs of barcode intervals matched in the most efficient way, whereas the other two are (i) the sum of all distances between barcode intervals matched in the most efficient way (Ws-distance) and (ii) pairs of persistent landscape functions matched from largest to smallest (Ls-distance) (see Supplementary Material text). The Btk-distance is therefore coarser and probably less efficient at capturing subtle information in protein structures. We also find that PH-distances in dimension 2 ($k=2$) are systematically smaller than those in dimension 1 ($k=1$) (Figs. S11 and S12), suggesting that cavities may be more conserved than cycles in protein structures.

Persistent homology captures strong phylogenetic signal in protein structures

To unravel the nature of the signal captured by PH, and in particular to determine the extent to which it is phylogenetic, we compared PH-distances (i.e. Btk-distances, Ws-distances, and Ls-distances) computed on structures for each of the 763,648 pairs of homologous proteins with evolutionary (EV)-distances calculated from Maximum likelihood trees (ML-distances) and multiple alignments (p -distances). The results show significant correlations ranging from 0.43 to 0.74 (all P -values < 0.008 , Table S2). The strongest correlations are observed with Ws-distances by applying AC filtrations (Fig. 2A and B), while the weakest correspond to Btk-distances computed from the VR filtration (Table S2).

Closer examination reveals five notable trends (Table S2). First, slightly higher correlations are observed with ML-distances than with p -distances ($r=0.44-0.74$ and $r=0.43-0.72$, respectively), the former being a better estimate of true evolutionary distances as it considers multiple substitutions in sequences. Second, the AC filtration provides stronger correlations than VR ($r=0.45-0.74$ and $r=0.43-0.67$, respectively). This may be because AC filtration is more appropriated to protein structures, as it considers local

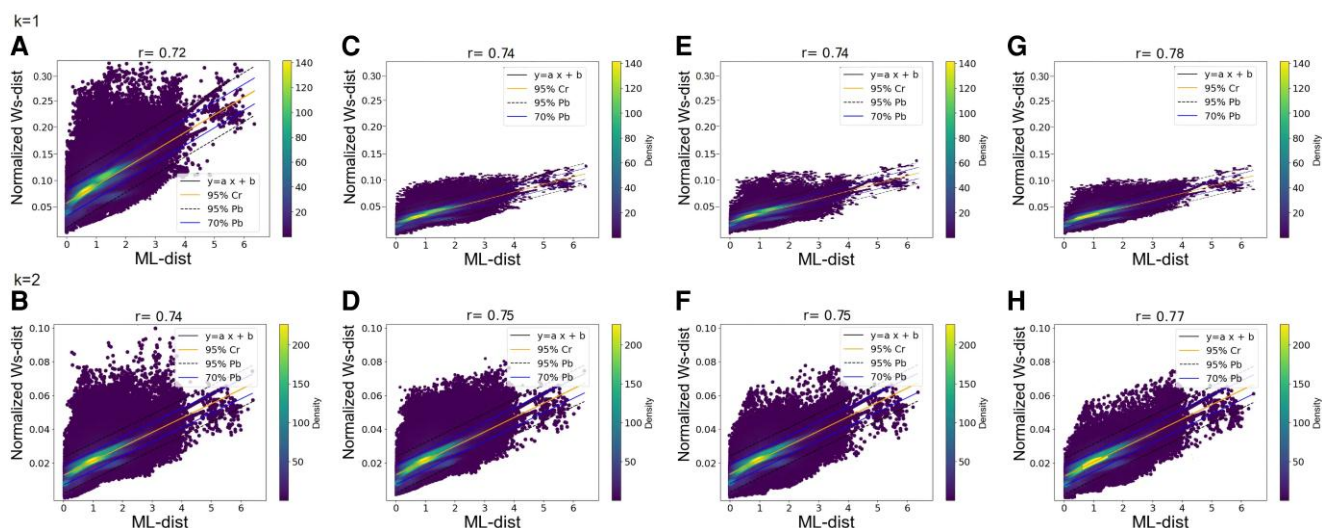


Fig. 2. Correlation plots between ML-distances and Ws-distances calculated by AC filtration on PC(α) of the AlphaFold2 predictions. Each plot contains 763,648 points, each corresponding to a pair of homologous proteins for which the ML-distance (x-axis) is compared with the normalized Ws-distance (y-axis). A) Normalized Ws-distances ($k = 1$) calculated on all α ($r = 0.72$, P -value = 5×10^{-4}), B) normalized Ws-distances ($k = 2$) calculated on all α ($r = 0.74$, P -value = 2×10^{-4}), C) as in A) except that the α corresponding to amino acid indels were omitted ($r = 0.74$, P -value = 3×10^{-5}), D) as in (B) except that the α corresponding to amino acid indels were omitted ($r = 0.75$, P -value = 7×10^{-4}), E) as in A) except that the α with CI < 70% were omitted ($r = 0.74$, P -value = 3×10^{-5}), F) as in B) except that the α with CI < 70% were omitted ($r = 0.75$, P -value = 6×10^{-4}), G) as in A) except that the α corresponding to amino acid indels and those with CI < 70% were omitted ($r = 0.76$, P -value = 9×10^{-4}), H) as in B) except that the α corresponding to amino acid indels and those with CI < 70% were omitted ($r = 0.77$, P -value = 6×10^{-4}). For details regarding confidence and prediction bands, see Fig. 1.

density within PCs to decide whether or not to connect two nearby points at each filtration step, whereas VR connects all pairs of points that come into contact, creating all corresponding simplexes (see [Supplementary Material](#) text). Third, the Ws-distance provides stronger correlations ($r = 0.63$ – 0.74) than the other two PH-distances ($r = 0.43$ – 0.66), whatever the homological dimension considered. This may reflect the fact that the Ws-distance considers all pairwise matched intervals, not just the most distant. It is therefore based on a more complete quantification of the information contained in barcodes than the Btk-distance and is better able to capture subtle differences in the geometry of the protein structures. Furthermore, while interval matching between barcodes is optimal for Ws-distances, the matching between persistent landscapes is not for Ls-distances. Fourth, PH-distances in dimensions 1 and 2 show similar correlations ($r = 0.44$ – 0.72 [$k = 1$] and $r = 0.43$ – 0.74 [$k = 2$]), suggesting that both cycles and cavities contain phylogenetic signal. Finally, we find significant correlations between the ML-distances and the PH-distances for the 518 protein families (ranging from 0.30 to 0.90) that cannot be observed by chance (Fig. S14), again demonstrating that PH allows a clear phylogenetic signal to be captured in structures.

Overall, our analysis reveals a strong correlation between PH-distances and EV-distances. This suggests that geometrical variations observed in structures correlate well with substitutions occurring in sequences and that the signal captured by PH in structures is mainly phylogenetic. We also show that PH-distances, particularly the Ws-distance computed from AC filtration, is most efficient at capturing this signal. Accordingly, in the following, we focused on Ws-distances calculated using the AC filtration.

Information carried by indels

Comparisons between PH-distances and EV-distances show a number of outliers corresponding to pairs of homologous proteins with unexpectedly high PH-distances (Fig. 2A and B). Close

examination of sequence alignments shows that the incriminated sequences contain large indels (see examples shown as Figs. S15–S20). In fact, we find that the correlation between PH-distances and EV-distances became weaker as the number of gaps in sequences being compared increased (Fig. S21). As expected, this is more pronounced when Ws-distances are compared with ML-distances, as these are derived from phylogenetic trees calculated after the alignment trimming step, which removes most of the indels in the sequences (Fig. S21A and B). Weaker but still significant correlations are also observed with p-distances, despite they are calculated on untrimmed multiple alignments (Fig. S21C and D).

To measure the contribution of indels, we computed Ws-distances by omitting α corresponding to amino acid indels. As expected, the correlation between PH-distances and EV-distances and the number of gaps in sequences disappears (Fig. S22). Overall, we observe a reduction in the dispersion around the regression line and a slight increase in the correlation coefficients with both ML-distances (from 0.72 to 0.74 [$k = 1$] and from 0.74 to 0.75 [$k = 2$], Fig. 2C and D) and p-distances (from 0.70 to 0.72 [$k = 1$] and from 0.72 to 0.74 [$k = 2$], not shown). This increase may seem modest, but it should be remembered that most of protein sequences studied here contain no or very few indels. If we consider only protein families whose sequences contain indels, the increase in correlations is much greater (from 0.70 to 0.74 [$k = 1$] and 0.69 to 0.76 [$k = 2$] for ML-distances and from 0.68 to 0.73 [$k = 1$] and 0.68 to 0.74 [$k = 2$] for p-distances). This suggests that indels in sequences generate a strong signal in protein structures that is efficiently captured by PH.

Effect of the quality of 3D structure predictions

We then asked to what extent the quality of structure prediction affects PH-distances. If protein structures do indeed contain a phylogenetic signal, we expect that the more realistic the predicted structures, the stronger the phylogenetic signal captured.

This is indeed the case as correlations between Ws-distances and ML-distances are stronger the higher the average C α CI of the structure predictions ($r = 0.50$, $P\text{-value} = 8 \times 10^{-5}$ [$k = 1$] and $r = 0.45$, $P\text{-value} = 2 \times 10^{-4}$ [$k = 2$]). Therefore, it would be interesting to investigate in more details whether correlations between PH-distances and EV-distances could be an indicator of the quality and the reliability of protein structure predictions. To go further, we calculated Ws-distances by considering only C α with a CI greater than or equal to 70%. We observe a slight increase in correlations with ML-distances from 0.72 to 0.74 ($k = 1$) and from 0.74 to 0.75 ($k = 2$) (Fig. 2A–E and B–F, respectively), meaning that amino acids with low CI, although few in numbers (6%), have an impact on the correlations between Ws-distances and ML-distances. These correlations reach 0.78 ($k = 1$) and 0.77 ($k = 2$) when C α corresponding to indels are also omitted (Fig. 2G and H).

Effect of genetic divergence within taxa on the intensity of the phylogenetic signal contained in protein structures

The 10 taxonomic groups studied cover a wide range of genetic divergence. This is illustrated by comparing the distribution of ML-distances between pairs of homologous protein sequences within each taxon (Fig. S23). In particular, medians of these distributions range from 0.02 for *Escherichia* to 1.53 for the *Bacteroidales*. As expected, due to the strong correlation between PH-distances and EV-distances highlighted above, Ws-distances are smaller for taxonomic groups with lower genetic divergence, whatever the homological dimension considered (Figs. S24 and S25). However, as structures are assumed to be more conserved than sequences, they are expected to contain a weaker phylogenetic signal, or even no signal when proteins are very similar at the sequence level. According to this hypothesis, we would expect correlations between Ws-distances and ML-distances to be weak for taxonomic groups with the lowest genetic diversity (e.g. *Escherichia*, *Thermococcales*, *Methanococcales*, *Enterobacterales*). We find that this is not the case (Fig. 3), implying that although structures evolve less rapidly than sequences, they contain a strong phylogenetic signal even at small evolutionary scale, which is efficiently captured by PH.

Comparison of the information carried by the different types of atoms in amino acids

So far, we focus on PC(C α), as it is expected to provide a good compromise between information and computation time (55). However, amino acids differ in the number, type and spatial organization of their side chain atoms (Figs. S26–S28). We therefore wonder to what extent focusing on C α might lead to a loss of information or introduce biases. We thus compared ML-distances with Ws-distances computed on PC(C α), PC(All-Atoms), PC(All-C), PC(All-N), and PC(All-O). We find that the correlations obtained with PC(C α) are higher ($r = 0.78$ [$k = 1$] and $r = 0.77$ [$k = 2$], Fig. 4A and B) than with PC(All-N), PC(All-O) and PC(All-C) ($r = 0.72$, 0.70, and 0.60 [$k = 1$] and $r = 0.68$, 0.66, and 0.56 [$k = 2$], respectively, Fig. 4C–H). This could suggest that PC(All-N), PC(All-O), and PC(All-C) contain a weaker phylogenetic signal, or more probably, reflects variations in the number of points in PCs. Indeed, the number of N, O, and C atoms in side chains varies depending on the amino acids considered (Figs. S26–S28). In the case of C α , variations in their number within PCs(C α) lead to a slight decrease in the correlation between PH-distances and ML-distances (see above). Accordingly, when considering O, N, or C atoms of side chains, similar effects are expected. In support of this hypothesis, the weakest correlation is observed for carbon atoms whose

number varies the most in side chains. This suggests that the signal due to variations in the number of O, N, and C atoms in side chains, is strong enough to partially obscure the phylogenetic signal contained in protein structures. Surprisingly, the correlations calculated using PC(All-Atoms) and PC(C α) are close ($r = 0.75$ and 0.78 [$k = 1$], and $r = 0.73$ and 0.77 [$k = 2$], Fig. 4A, B, I, and J). One hypothesis would be that the combination of the strong phylogenetic signal contained in PC(C α), and to a lesser extent in PC(All-N) and PC(All-O), compensates for the noise associated with high variations in the number of C atoms in the side chains.

Discussion and conclusion

Studying the historical information contained in protein sequences has limitations especially when sequences are highly divergent (11, 62). In that context, structures have been proposed as an alternative to sequences, as they are assumed to evolve slower (6, 12, 17). Until now, their use for phylogenetic inference has been limited by the absence or the insufficient number of structures available for most protein families. This is about to change, thanks to the development of methods based on artificial intelligence that allow virtually unlimited access to protein structures (63). This is opening up a new era in structural biology and paves the way for using structures in all fields of life sciences (64, 65), including the study of protein evolution (15). However, translating structural distances into evolutionary information remain a challenge by the lack of models allowing to bridge the gap between protein structure and sequence evolution (18, 66, 67).

This work, which aims to explore new ways of capturing the signal contained in structures, is part of that dynamic. Here, we investigate the potential of PH, an original approach from the topological data analysis, to capture a phylogenetic signal from protein structures. PH allows protein structures, represented as PCs, to be compared according to their intrinsic geometric characteristics, in particular the presence of cycles (in homological dimension 1) and cavities (homological dimension 2) formed by the position of their amino acid atoms in 3D space. The originality of PH is that it does not rely on direct structures comparisons. Indeed, PH proposes an algebraic formalism for measuring the geometric features of 3D representations by abstracting their multiscale organization through a structure filtration algorithm. In this way, the entire structure of the protein is considered and, unlike most approaches, PH avoids the need to align structures, a critical step in most analyses (16, 39). One of the major advantages of PH is that PH-descriptors are invariant to small variations in the coordinates of points in PCs. Therefore, PH allows the study of dynamical entities, such as protein structures, from one of their static representations. This good stability of the descriptors results from the fact that the geometric characteristics of a structure are calculated from a filtration of its PC representation along a gradient of spatial scales. This filtration progressively links points within the PC. Intrinsic geometric features of the PC will persist significantly along this filtration, while those resulting from small variations will be ephemeral and will not be considered to compute PH-distances. This property allows to limit the effect of microvariations in the coordinates of the atoms due to the dynamical nature of protein structures (i.e. slight topological oscillations and variations) and atomic uncertainties in the coordinates of atoms in bioinformatically predicted or experimentally solved protein structures.

Examination of a large dataset consisting of 518 protein families, representing more than 700,000 pairs of homologous proteins, reveals a strong and significant linear relationship between distances computed on protein sequences and

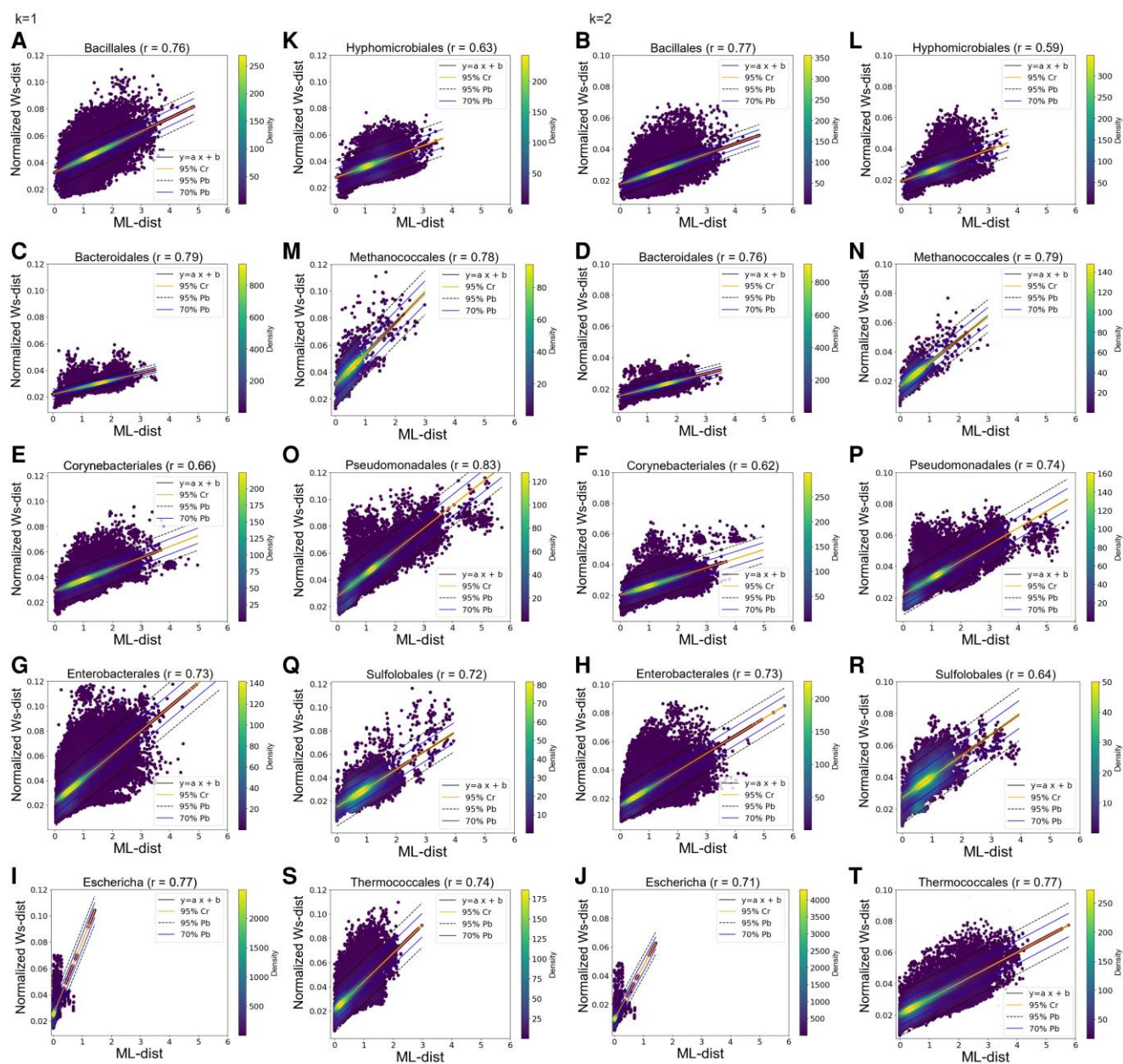


Fig. 3. Correlation plots between ML-distances and Ws-distances computed for each of the 10 taxa. On a given plot, each dot corresponds to a pair of homologous proteins for which the ML-distance (x-axis) is compared to the normalized Ws-distance computed on PC(Ca with $CI > 70\%$) when indels are omitted (y-axis). All P-values are less than 4×10^{-5} . A) *Bacillales*: 170,354 pairs of homologous proteins ($k = 1$), B) *Bacillales*: 170,354 pairs of homologous proteins ($k = 2$), C) *Bacteroidales*: 40,402 pairs of homologous proteins ($k = 1$), D) *Bacteroidales*: 40,402 pairs of homologous proteins ($k = 2$), E) *Corynebacteriales*: 154,513 pairs of homologous proteins ($k = 1$), F) *Corynebacteriales*: 40,402 pairs of homologous proteins ($k = 2$), G) *Enterobacteriales*: 196,915 pairs of homologous proteins ($k = 1$), H) *Enterobacteriales*: 196,915 pairs of homologous proteins ($k = 2$), I) *Escherichia*: 23,879 pairs of homologous proteins ($k = 1$), J) *Escherichia*: 23,879 pairs of homologous proteins ($k = 2$), K) *Hyphomicrobiales*: 38,679 pairs of homologous proteins ($k = 1$), L) *Hyphomicrobiales*: 38,679 pairs of homologous proteins ($k = 2$), M) *Methanococcales*: 2,711 pairs of homologous proteins ($k = 1$), N) *Methanococcales*: 2,711 pairs of homologous proteins ($k = 2$), O) *Pseudomonadales*: 75,834 pairs of homologous proteins ($k = 1$), P) *Pseudomonadales*: 75,834 pairs of homologous proteins ($k = 2$), Q) *Sulfolobales*: 11,453 pairs of homologous proteins ($k = 1$), R) *Sulfolobales*: 11,453 pairs of homologous proteins ($k = 2$), S) *Thermococcales*: 48,908 pairs of homologous proteins ($k = 1$), T) *Thermococcales*: 48,908 pairs of homologous proteins ($k = 2$). For details regarding confidence and prediction bands, see Fig. 1.

structures in both homological dimensions 1 and 2. This means that variations in the geometry of structures measured by the persistence of cycles and cavities constitute a strong phylogenetic signal that is efficiently captured by PH. Furthermore, PH is a very sensitive method, as it detects the phylogenetic signal even when the proteins studied are very similar at the sequence level (i.e. differing by only a few amino acids), as well as when they are very divergent (i.e. differing in average by more than two to

four substitutions per site). However, we also observe that the strength of this correlation varies among the 518 families of homologous proteins analyzed. This agrees with previous reports (12, 68). The next step will be to determine which factors may be responsible for the discrepancies between PH-distances and evolutionary distances. For example, it has been proposed that (i) sequences may follow a structurally constrained neutral evolution, which allow sequences to evolve freely as long as

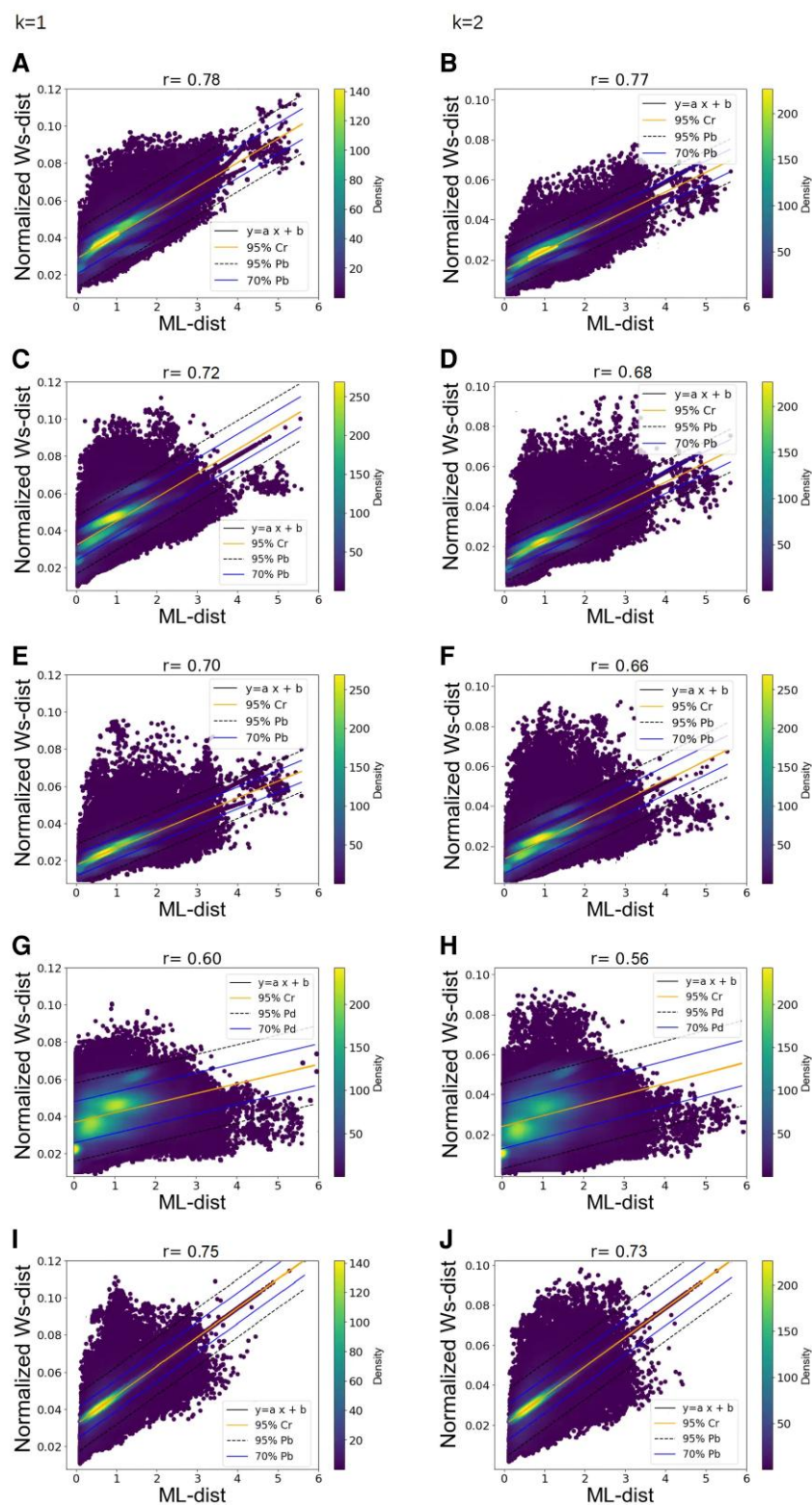


Fig. 4. Correlation plots between ML-distances and Ws-distances according to the type of considered atoms. Each plot contains 763,648 points, each corresponding to a pair of homologous proteins for which the ML-distance (x-axis) is compared to the normalized Ws-distance (y-axis). To calculate distances, atoms corresponding to amino acids whose Ca CI > 70% or corresponding to indel were omitted. All P-values are less than 3×10^{-4} A) PC(Ca) ($k = 1$), B) PC(Ca) ($k = 2$), C) PC(All-N) ($k = 1$), D) PC(All-N) ($k = 2$), E) PC(All-O) ($k = 1$), F) PC(All-O) ($k = 2$), G) PC(All-C) ($k = 1$), H) PC(All-C) ($k = 2$), I) PC(All-Atoms) ($k = 1$), J) PC(All-Atoms) ($k = 2$). For details regarding confidence and prediction bands, see Fig. 1.

the structure is preserved (67, 69–72), (ii) that protein interactions may constrain the evolution of structures (73), or (iii) that duplication, transfer and recombination of short protein segments may

have played an important role in the evolution of structures, leading to local areas of similarity within proteins or even between distant proteins (74–77).

Previous studies have shown that amino acid insertions and deletions in protein sequences could impact deeply protein structure (78–80). For example, although they are rarer than amino acids substitutions, they could account for more than 45% of structural variation (81). Although we confirm the effect of deletions and insertions on the differences observed between the distances calculated from sequences and from structures, this effect remains relatively weak. This may reflect the fact that the different studies are not based on the same sets of proteins and/or that PH is intrinsically less sensitive to the effect of amino acid insertions and deletions in proteins than other methods because it measures variations in the geometric properties of proteins rather than overall changes in protein shapes. This issue requires further investigation. To limit the biases, it has been proposed to remove the amino acids corresponding to indels from structures before calculating distances (17) or to normalize distances (82, 83). A key question is whether to include indels or leave them out, as most studies based on sequence comparison do. There is no easy answer to this question. If indels result from sequencing, assembly, or annotation errors, including them will lead to an overestimation of evolutionary distances. In this case, omitting the atoms of the incriminating amino acids can easily overcome this problem. On the other hand, if they are the result of true evolutionary events, ignoring them will lead to an underestimation of the evolutionary distances between proteins.

We observe also that not all the atoms in the structures carry the same information. While the use of C α atoms was sufficient to capture a strong phylogenetic signal in structures, using N, O, and C atoms of side chains atoms turned out to be less efficient. The extent to which the signal carried by the atoms in the amino acid side chains is noisy or informative will require further investigations. For example, it has been shown that environmental factors, such as temperature or salinity, exert very strong constraints on proteins, resulting in variations in the frequency of each type of amino acid in protein sequences (84–88). We expect these constraints to be associated with specific signatures in protein structures that can be revealed by PH.

Refining the algorithms underlying the PH method represents our next goal. Although filtration methods and PH-distances used in this study can capture the phylogenetic information contained in protein structures, they were not specifically designed to analyze this type of information. In particular, they do not incorporate information about how proteins evolve, as do models used to calculate evolutionary distances between sequences. Filling this gap will require filtration algorithms that consider additional information such as the nature and the physicochemical features of amino acids, which represents a promising direction for the future development of topological analysis in phylogenetics. Finally, another line of research is exploring the potential contribution of approaches combining PH with machine learning to study protein structure evolution, as PH has been shown to significantly improve classical machine learning (89, 90). Indeed, PH-descriptors provide vectorizations of the complex geometry of protein structures, facilitating the application of learning methods. The application of such approaches has proven to be very efficient for protein classification (60) and protein engineering (91). We show here that PH-descriptors can be used to capture the phylogenetic signal, paving the way for the development of new approaches to study the evolution of protein based on their geometric structure.

Materials and methods

A detail scheme of the pipeline used is shown as Fig. 5.

Dataset assembly

The study has been conducted on seven bacterial and three archaeal major taxa: *Bacillales* (Firmicutes), *Bacteroidales* (CFB group bacteria), *Corynebacteriales* (Actinomycetota), *Enterobacterales* and *Pseudomonadales* (Gammaproteobacteria), *Hyphomicrobiales* (Alphaproteobacteria), *Escherichia* (*Enterobacterales*), *Methanococcales* (*Euryarchaeotes*), *Thermococcales* (*Euryarchaeotes*), and *Sulfolobales* (*Crenarchaeotes*). Reference and representative proteomes of these groups were retrieved from the RefSeq database at the National Center for Biotechnology Information (92). When the number of available proteomes was high for a given taxon, a subsampling of 100 proteomes representative of its diversity has been performed (Table S3).

For each taxon, experimentally resolved structures of monomeric proteins were extracted from the RCSB PDB (93). To ensure the quality of structural data, we considered protein with structures resolution <1.5 Å for bacteria and <2 Å for archaea (see Supplementary Material text). We did not perform an exhaustive analysis of all structures available in the PDB, as our aim was to analyze a significant but reasonable number of protein families with at least one experimentally well resolved protein 3D structure in the PDB. For Archaea, due to their limited number, we considered all structures with a resolution below 2 Å. Applying such a criterion to the seven studied bacterial groups would have resulted in a huge number of proteins, and thus protein families, requiring a huge (and perhaps unnecessary) number of 3D structure predictions. That's why we only considered the structures with the best resolution. To avoid redundancy, when several structures were available for a given protein, the one with the best resolution was kept.

For each protein, the corresponding family of homologous proteins was assembled as follows. Homologs were identified in members of the taxon to which the protein belongs using the BLASTP program (94). Alignments with e-value <10⁻³, amino acid identity >0.3, query and subject coverages >0.8, and gap content <0.1 were considered as significant, and the corresponding sequences were retrieved. Protein families containing <7 homologous sequences were discarded.

The final dataset represents 518 protein families, corresponding to 22,940 protein sequences and 763,648 pairs of homologous sequences (Tables S4–S13).

Protein 3D structure modeling

The structures of the 22,940 proteins were computed with AlphaFold2 using the NMRbox (19). We retained predicted models with the highest quality score.

Point cloud filtration

For each modeled structure, we defined five PCs corresponding to the 3D coordinates of amino acid atoms: alpha carbon (PC(C α)), all atoms (PC(All-Atoms)), all carbon (PC(All-C)), all nitrogen (PC(All-N)), and all oxygen (PC(All-O)). The Vietoris-Rips (VR) and Alpha Complex (AC) filtration algorithms, and PH-descriptors (i.e. barcodes and persistent landscapes) in homological dimensions 1 and 2 ($k = 1$ and $k = 2$, respectively), were computed using the GUDHI library (95). We have not considered PH-descriptors in homological dimension 0, as they reflect mainly the distances between points and not the intrinsic geometrical properties of PCs.

Phylogenetic inference and computation of evolutionary distances

For each protein family, an accurate multiple alignment was built using MAFFT v7.453 with the L-INSI option (96) and trimmed using

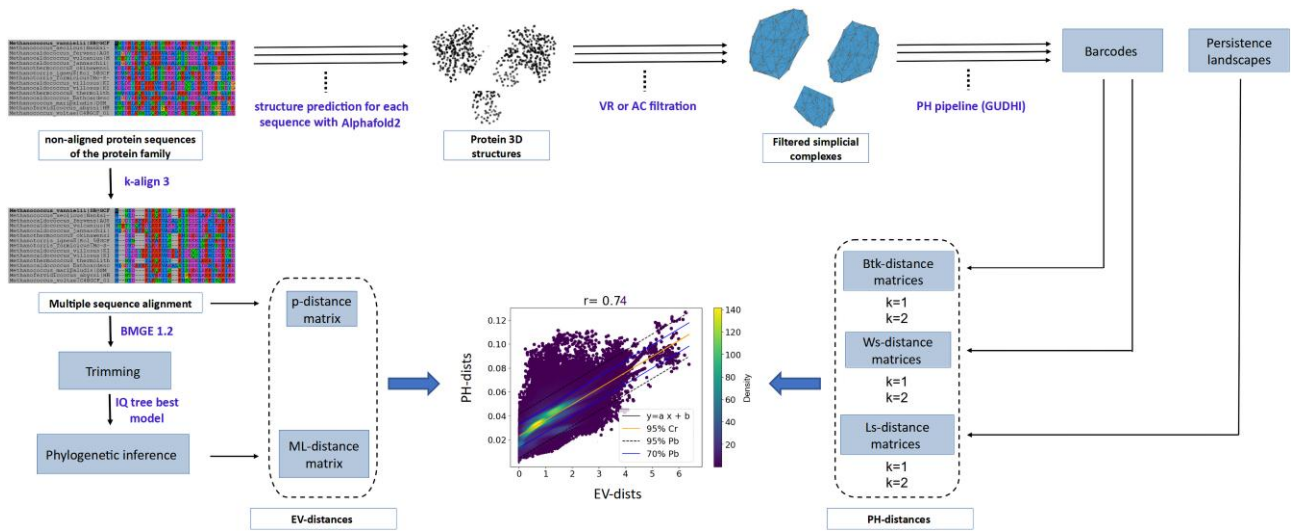


Fig. 5. Pipeline describing the steps for the comparison of EV- and PH-distances on each of the 518 protein families. We start by predicting the structure of each sequence in the protein family using AlphaFold2. Atoms coordinates constitute the PC on which we apply VR or AC filtration to obtain filtered simplicial complexes. By computing the PH of each obtained filtered simplicial complexes, we generate four PH-descriptors (two barcodes and two persistence landscapes) in homological dimension 1 and 2 ($k=1$ and $k=2$, respectively). For each pair of structures, the barcodes are compared using Btk-distances and Ws-distances in each dimension, and the persistence landscapes are compared using Ls-distances. This generated six PH-distance matrices. On the other hand, we align the protein family and compute the p-distance matrix between each pair of sequences. After trimming the multiple sequence alignment, we infer the phylogenetic tree and compute from it the ML-distance matrix. Each EV-distance matrix is then compared to each PH-distance matrix.

BMGE v2 with the BLOSUM45 substitution matrix (97). A maximum likelihood (ML) phylogenetic tree was inferred using IQ-TREE v2.1.2 (98) and the best fitted-model according to ModelFinder (99). The tree branch robustness was estimated using the ultrafast bootstrap procedure implemented in IQ-TREE (1,000 replicates). For each pair of sequences, EV-distances were computed using SEAVIEW v5.0.5 (100). More precisely, observed distances (p -distances) were computed from the untrimmed multiple alignments, while ML-distances correspond to patristic distances computed from the ML-trees.

PH-distance definitions and computation

For each protein family, we calculate a matrix of PH-distances between pairs of homologous protein structures. The PH-distances between two structures are calculated from the associated barcodes in homological dimensions 1 and 2 ($k=1$ and $k=2$) (see [Supplementary Material](#) text for more details). These distances are defined as follows:

The bottleneck distance (Btk1, Btk2) between two barcodes P and Q is defined by

$$\text{Btk}(P, Q) = \inf_{\varphi: P \rightarrow Q} \sup_{a \in P} \|a - \varphi(a)\|_{\infty},$$

where φ ranges over all bijections between P and Q and a is an interval in P .

The Wasserstein distance (Ws1, Ws2) between two barcodes P and Q is defined by

$$\text{Ws}(P, Q) = \inf_{\varphi: P \rightarrow Q} \sqrt{\sum_{a \in P} \|a - \varphi(a)\|_2^2},$$

where the infimum is taken over all bijections φ between P and Q .

The Landscape distance (Ls1, Ls2) between two persistence landscapes λ, λ' is given by the L^2 -norm:

$$\text{Ls}(\lambda, \lambda') = \sqrt{\sum_{\ell=1}^{\infty} \int |\lambda_{\ell}(t) - \lambda'_{\ell}(t)|^2 dt}.$$

The Btk1, Btk2, Ws1, and Ws2 distances were computed using the GUDHI library (95), while Landscape distances (Ls1, Ls2) were computed using Pysistence (61). We used $p=2$ for Ls1 and Ls2 and $p=q=2$ for Ws1 and Ws2 (see [Supplementary Material](#) text). The Pearson's coefficient correlation was used to calculate the correlation between EV-distances and PH-distances.

To go further, we tested the impact of three protein features on PH-distances: (i) the length of the proteins, (ii) the amount of indels in protein sequences, and (iii) the quality of predicted structures. Regarding protein length, to enable comparisons between different datasets, phylogenetic distances computed from molecular sequences are usually normalized by the number of compared residues (i.e. amino acid or nucleotide sites) and expressed in unit of expected number of substitutions per site. This allows to compare distances computed from protein of different lengths. In contrast, PH-distances are not normalized, which precludes comparisons of PH-distances computed from PCs with different number of points, and thus of structures with different number of amino acids/atoms. To overcome this issue, we normalized PH-distances by the average number of points of the two compared PCs (see [Supplementary Material](#) text). Regarding indels, starting from the multiple sequences alignments, we identified the amino acids involved in indels for each pair of proteins. Their atoms were omitted for the calculation of PH-distances from PCs. Therefore, for each structure, the number of atoms considered varies depending on the structure it is compared to (see [Supplementary Material](#) text). Finally, to measure the impact of structure prediction quality, we masked points corresponding to amino acids having an index lower than 70% in PCs (see [Supplementary Material](#) text).

Acknowledgments

We would like to thank the P2HPD computing center hosted by Université Claude Bernard Lyon 1. We acknowledge Federico Napoli from the Institute of Science and Technology Austria

(ISTA), Umberto Lupo from École Polytechnique Fédérale de Lausanne (EPFL) for useful suggestions and stimulating discussion. We also thank Jean-Pierre Flandrois and Rémi-Vinh Coudert from the Laboratory of Biometry and Evolutionary Biology (LBEB) for their constructive opinions and very helpful recommendations, as well as Fida El Chami from the Lebanese University and Joseph Nardin-Gennequin from Claude Bernard University for their valuable advices and fruitful discussions.

Supplementary Material

Supplementary material is available at PNAS Nexus online.

Funding

L.B.D. was supported by SAFAR scholarship funded by the Institut Français and Université Libanaise (129638R). This work has been supported by the French National Research Agency (ANR-22-CE02-0027).

Author Contributions

L.B.D.: data curation; formal analysis; investigation; methodology; writing-original draft; writing-review and editing. D.M.: conceptualization; writing-original draft; writing-review and editing. P.M.: conceptualization; supervision; funding acquisition; investigation; methodology; writing-original draft; writing-review and editing. C.B.-A.: conceptualization; supervision; funding acquisition; investigation; methodology; writing-original draft; writing-review and editing.

Data Availability

Protein sequences, multiple alignments, ML trees, and 3D protein structure predictions were deposited in the permanent Mendeley data repository [<https://data.mendeley.com/datasets/mhprc6c827/1>] (DOI 10.17632/mhprc6c827.1) (101).

References

- 1 Kapli P, Yang Z, Telford MJ. 2020. Phylogenetic tree building in the genomic age. *Nat Rev Genet.* 21(7):428–444.
- 2 Steenwyk JL, Li Y, Zhou X, Shen XX, Rokas A. 2023. Incongruence in the phylogenomics era. *Nat Rev Genet.* 24(12):834–850.
- 3 Delsuc F, Brinkmann H, Philippe H. 2005. Phylogenomics and the reconstruction of the tree of life. *Nat Rev Genet.* 6(5):361–375.
- 4 Rodrigue N, Lartillot N, Bryant D, Philippe H. 2005. Site interdependence attributed to tertiary structure in amino acid sequence evolution. *Gene.* 347(2):207–217.
- 5 Larson G, Thorne JL, Schmidler S. 2020. Incorporating nearest-neighbor site dependence into protein evolution models. *J Comput Biol.* 27(3):361–375.
- 6 Herman JL, Challis CJ, Novak A, Hein J, Schmidler SC. 2014. Simultaneous Bayesian estimation of alignment and phylogeny under a joint model of protein sequence and structure. *Mol Biol Evol.* 31(9):2251–2266.
- 7 Challis CJ, Schmidler SC. 2012. A stochastic evolutionary model for protein structure alignment and phylogeny. *Mol Biol Evol.* 29(11):3575–3587.
- 8 Nagar N, Ben Tal N, Pupko T. 2022. Evorator: prediction of residue-level evolutionary rates from protein structures using machine learning. *J Mol Biol.* 434(11):167538.

- 9 Loewenthal G, et al. 2021. A probabilistic model for indel evolution: differentiating insertions from deletions. *Mol Biol Evol.* 38(12):5769–5781.
- 10 Trost J, et al. 2024. Simulations of sequence evolution: how (un) realistic they are and why. *Mol Biol Evol.* 41(1):msad277.
- 11 Gribaldo S, Philippe H. 2002. Ancient phylogenetic relationships. *Theor Popul Biol.* 61(4):391–408.
- 12 Illergard K, Ardell DH, Elofsson A. 2009. Structure is three to ten times more conserved than sequence—a study of structural response in protein cores. *Proteins.* 77(3):499–508.
- 13 Qi Y, Grishin NV. 2005. Structural classification of thioredoxin-like fold proteins. *Proteins.* 58(2):376–388.
- 14 Lundin D, Poole AM, Sjoberg BM, Hogborn M. 2012. Use of structural phylogenetic networks for classification of the ferritin-like superfamily. *J Biol Chem.* 287(24):20565–20575.
- 15 Holm L, Laiho A, Toronen P, Salgado M. 2023. Dali shines a light on remote homologs: one hundred discoveries. *Protein Sci.* 32(1):e4519.
- 16 Hasegawa H, Holm L. 2009. Advances and pitfalls of protein structural alignment. *Curr Opin Struct Biol.* 19(3):341–348.
- 17 Malik AJ, Poole AM, Allison JR. 2020. Structural phylogenetics with confidence. *Mol Biol Evol.* 37(9):2711–2726.
- 18 Herman JL. 2019. Enhancing statistical multiple sequence alignment and tree inference using structural information. *Methods Mol Biol.* 1851:183–214.
- 19 Jumper J, et al. 2021. Highly accurate protein structure prediction with AlphaFold. *Nature.* 596(7873):583–589.
- 20 Varadi M, et al. 2024. Alphafold protein structure database in 2024: providing structure coverage for over 214 million protein sequences. *Nucleic Acids Res.* 52(D1):D368–D375.
- 21 Koehler Leman J, et al. 2023. Sequence-structure-function relationships in the microbial protein universe. *Nat Commun.* 14(1):2351.
- 22 Choi IG, Kwon J, Kim SH. 2004. Local feature frequency profile: a method to measure structural similarity in proteins. *Proc Natl Acad Sci USA.* 101(11):3797–3802.
- 23 Budowski-Tal I, Nov Y, Kolodny R. 2010. Fragbag, an accurate representation of protein structure, retrieves structural neighbors from the entire PDB quickly and accurately. *Proc Natl Acad Sci U S A.* 107(8):3481–3486.
- 24 Xia C, Feng SH, Xia Y, Pan X, Shen HB. 2022. Fast protein structure comparison through effective representation learning with contrastive graph neural networks. *PLoS Comput Biol.* 18(3):e1009986.
- 25 Krissinel E, Henrick K. 2004. Secondary-structure matching (SSM), a new tool for fast protein structure alignment in three dimensions. *Acta Crystallogr D Biol Crystallogr.* 60(Pt 12 Pt 1):2256–2268.
- 26 Zhang Y, Skolnick J. 2005. TM-align: a protein structure alignment algorithm based on the TM-score. *Nucleic Acids Res.* 33(7):2302–2309.
- 27 Holm L, Sander C. 1995. Dali: a network tool for protein structure comparison. *Trends Biochem Sci.* 20(11):478–480.
- 28 Zhang C, Shine M, Pyle AM, Zhang Y. 2022. US-align: universal structure alignments of proteins, nucleic acids, and macromolecular complexes. *Nat Methods.* 19(9):1109–1115.
- 29 Mirzaei S, Razmara J, Lotfi S. 2021. GADP-align: a genetic algorithm and dynamic programming-based method for structural alignment of proteins. *Bioimpacts.* 11(4):271–279.
- 30 Zotenko E, O’Leary DP, Przytycka TM. 2006. Secondary structure spatial conformation footprint: a novel method for fast protein structure comparison and classification. *BMC Struct Biol.* 6:12.

- 31 Rogen P, Fain B. 2003. Automatic classification of protein structure by using Gauss integrals. *Proc Natl Acad Sci USA*. 100(1):119–124.
- 32 Bale A, Rambo R, Prior C. 2023. The SKMT algorithm: a method for assessing and comparing underlying protein entanglement. *PLoS Comput Biol*. 19(11):e1011248.
- 33 van Kempen M, et al. 2024. Fast and accurate protein structure search with Foldseek. *Nat Biotechnol*. 42(2):243–246.
- 34 Shindyalov IN, Bourne PE. 1998. Protein structure alignment by incremental combinatorial extension (CE) of the optimal path. *Protein Eng*. 11(9):739–747.
- 35 Daniluk P, Oleniecki T, Lesyng B. 2021. DAMA: a method for computing multiple alignments of protein structures using local structure descriptors. *Bioinformatics*. 38(1):80–85.
- 36 Shegay MV, Suplatov DA, Popova NN, Svedas VK, Voevodin VV. 2019. parMATT: parallel multiple alignment of protein 3D-structures with translations and twists for distributed-memory systems. *Bioinformatics*. 35(21):4456–4458.
- 37 Akdel M, Durairaj J, de Ridder D, van Dijk ADJ. 2020. Caretta—a multiple protein structure alignment and feature extraction suite. *Comput Struct Biotechnol J*. 18:981–992.
- 38 Breitling R, Laubner D, Adamski J. 2001. Structure-based phylogenetic analysis of short-chain alcohol dehydrogenases and reclassification of the 17 β -hydroxysteroid dehydrogenase family. *Mol Biol Evol*. 18(12):2154–2161.
- 39 Kolodny R, Koehl P, Levitt M. 2005. Comprehensive evaluation of protein structure alignment methods: scoring by geometric measures. *J Mol Biol*. 346(4):1173–1188.
- 40 Romei M, et al. 2022. Protein folds as synapomorphies of the tree of life. *Evolution*. 76(8):1706–1719.
- 41 Deeds EJ, Shakhnovich EI. 2007. A structure-centric view of protein evolution, design, and adaptation. *Adv Enzymol Relat Areas Mol Biol*. 75:133–191. xi–xii.
- 42 Wolf YI, Brenner SE, Bash PA, Koonin EV. 1999. Distribution of protein folds in the three superkingdoms of life. *Genome Res*. 9(1):17–26.
- 43 Carlsson G. 2009. Topology and data. *Bull Am Math Soc*. 46(2):255–308.
- 44 Nicolau M, Levine AJ, Carlsson G. 2011. Topology based data analysis identifies a subgroup of breast cancers with a unique mutational profile and excellent survival. *Proc Natl Acad Sci USA*. 108(17):7265–7270.
- 45 Iqbal Z, Gandhi SD, Kersten JR, Pagel PS. 2007. An unusual right atrial structure in a patient with a new diastolic murmur. *J Cardiothorac Vasc Anesth*. 21(1):152–154.
- 46 Lawson P, Sholl AB, Brown JQ, Fasy BT, Wenk C. 2019. Persistent homology for the quantitative evaluation of architectural features in prostate cancer histology. *Sci Rep*. 9(1):1139.
- 47 Vandaele R, Mukherjee P, Selby HM, Shah RP, Gevaert O. 2023. Topological data analysis of thoracic radiographic images shows improved radiomics-based lung tumor histology prediction. *Patterns (N Y)*. 4(1):100657.
- 48 Li M, et al. 2018. The persistent homology mathematical framework provides enhanced genotype-to-phenotype associations for plant morphology. *Plant Physiol*. 177(4):1382–1395.
- 49 Amezcuita EJ, Quigley MY, Ophelders T, Munch E, Chitwood DH. 2020. The shape of things to come: topological data analysis and biology, from molecules to organisms. *Dev Dyn*. 249(7):816–833.
- 50 Meng Z, Anand DV, Lu Y, Wu J, Xia K. 2020. Weighted persistent homology for biomolecular data analysis. *Sci Rep*. 10(1):2079.
- 51 Duman AN, Pirim H. 2018. Gene coexpression network comparison via persistent homology. *Int J Genomics*. 2018:7329576.
- 52 Cohen-Steiner D, Edelsbrunner H, Harer J. 2006. Stability of persistence diagrams. *Discrete Comput Geom*. 37(1):103–120.
- 53 Ichinomiya T, Obayashi I, Hiraoka Y. 2020. Protein-Folding analysis using features obtained by persistent homology. *Biophys J*. 118(12):2926–2937.
- 54 Kovacev-Nikolic V, Bubenik P, Nikolic D, Heo G. 2016. Using persistent homology and dynamical distances to analyze protein binding. *Stat Appl Genet Mol Biol*. 15(1):19–38.
- 55 Xia K, Wei GW. 2014. Persistent homology analysis of protein structure, flexibility, and folding. *Int J Numer Method Biomed Eng*. 30(8):814–844.
- 56 Wei X, Chen J, Wei GW. 2023. Persistent topological Laplacian analysis of SARS-CoV-2 variants. *J Comput Biophys Chem*. 22(5):569–587.
- 57 Bi J, et al. 2023. Multiscale topological indices for the quantitative prediction of SARS CoV-2 binding affinity change upon mutations. *J Chem Inf Model*. 63(13):4216–4227.
- 58 Qiu Y, Wei GW. 2023. Persistent spectral theory-guided protein engineering. *Nat Comput Sci*. 3(2):149–163.
- 59 Hamilton W, Borgert JE, Hamelryck T, Marron JS. 2022. Persistent topology of protein space. In: Gasparovic E, Robins V, Turner K, editors. *Research in computational topology 2*. Cham (Switzerland): Springer International Publishing. p. 233–244.
- 60 Cang Z, et al. 2015. A topological approach for protein classification. *Mol Based Math Biol*. 3(1):140–162.
- 61 Benjamin K, et al. 2023. Homology of homologous knotted proteins. *J R Soc Interface*. 20(201):20220727.
- 62 Delsuc F, Baurain D, Philippe H. 2006. Vertebrate origins: does the tunic make the man? *Med Sci (Paris)*. 22(8–9):688–690.
- 63 Lupas AN, et al. 2021. The breakthrough in protein structure prediction. *Biochem J*. 478(10):1885–1890.
- 64 Masrati G, et al. 2021. Integrative structural biology in the era of accurate structure prediction. *J Mol Biol*. 433(20):167127.
- 65 Bordin N, et al. 2023. Novel machine learning approaches revolutionize protein knowledge. *Trends Biochem Sci*. 48(4):345–359.
- 66 Liberles DA, et al. 2012. The interface of protein structure, protein biophysics, and molecular evolution. *Protein Sci*. 21(6):769–785.
- 67 Worth CL, Gong S, Blundell TL. 2009. Structural and functional constraints in the evolution of protein families. *Nat Rev Mol Cell Biol*. 10(10):709–720.
- 68 Panchenko AR, Wolf YI, Panchenko LA, Madej T. 2005. Evolutionary plasticity of protein families: coupling between sequence and structure variation. *Proteins*. 61(3):535–544.
- 69 Gilson AI, Marshall-Christensen A, Choi JM, Shakhnovich EI. 2017. The role of evolutionary selection in the dynamics of protein structure evolution. *Biophys J*. 112(7):1350–1365.
- 70 Sadowski MI, Taylor WR. 2010. On the evolutionary origins of “Fold Space Continuity”: a study of topological convergence and divergence in mixed alpha-beta domains. *J Struct Biol*. 172(3):244–252.
- 71 Choi SC, Hobolth A, Robinson DM, Kishino H, Thorne JL. 2007. Quantifying the impact of protein tertiary structure on molecular evolution. *Mol Biol Evol*. 24(8):1769–1782.
- 72 Kleinman CL, Rodrigue N, Lartillot N, Philippe H. 2010. Statistical potentials for improved structurally constrained evolutionary models. *Mol Biol Evol*. 27(7):1546–1560.
- 73 Naveenkumar N, Prabantu VM, Vishwanath S, Sowdhamini R, Srinivasan N. 2022. Structures of distantly related interacting protein homologs are less divergent than non-interacting homologs. *FEBS Open Bio*. 12(12):2147–2153.

- 74 Eck RV, Dayhoff MO. 1966. Evolution of the structure of ferredoxin based on living relics of primitive amino acid sequences. *Science*. 152(3720):363–366.
- 75 Qiu K, Ben-Tal N, Kolodny R. 2022. Similar protein segments shared between domains of different evolutionary lineages. *Protein Sci*. 31(9):e4407.
- 76 Romero Romero ML, Rabin A, Tawfik DS. 2016. Functional proteins from short peptides: Dayhoff's hypothesis turns 50. *Angew Chem Int Ed Engl*. 55(52):15966–15971.
- 77 Kolodny R. 2021. Searching protein space for ancient subdomain segments. *Curr Opin Struct Biol*. 68:105–112.
- 78 Miton CM, Tokuriki N. 2023. Insertions and deletions (indels): a missing piece of the protein engineering jigsaw. *Biochemistry*. 62(2):148–157.
- 79 Toth-Petroczy A, Tawfik DS. 2013. Protein insertions and deletions enabled by neutral roaming in sequence space. *Mol Biol Evol*. 30(4):761–771.
- 80 Jilani M, Turcan A, Haspel N, Jagodzinski F. 2022. Elucidating the structural impacts of protein InDels. *Biomolecules*. 12(10):1435.
- 81 Zhang Z, Wang J, Gong Y, Li Y. 2018. Contributions of substitutions and indels to the structural variations in ancient protein superfamilies. *BMC Genomics*. 19(1):771.
- 82 Carugo O, Pongor S. 2001. A normalized root-mean-square distance for comparing protein three-dimensional structures. *Protein Sci*. 10(7):1470–1473.
- 83 Saberi Fathi SM. 2016. A new definition and properties of the similarity value between two protein structures. *J Biol Phys*. 42(4):621–636.
- 84 Lecocq M, Groussin M, Gouy M, Brochier-Armanet C. 2021. The molecular determinants of thermoadaptation: methanococcales as a case study. *Mol Biol Evol*. 38(5):1761–1776.
- 85 Amangeldina A, Tan ZW, Berezovsky IN. 2024. Living in trinity of extremes: genomic and proteomic signatures of halophilic, thermophilic, and pH adaptation. *Curr Res Struct Biol*. 7:100129.
- 86 Paul S, Bag SK, Das S, Harvill ET, Dutta C. 2008. Molecular signature of hypersaline adaptation: insights from genome and proteome composition of halophilic prokaryotes. *Genome Biol*. 9(4):R70.
- 87 Boussau B, Blanquart S, Necsulea A, Lartillot N, Gouy M. 2008. Parallel adaptations to high temperatures in the Archaeal eon. *Nature*. 456(7224):942–945.
- 88 Zeldovich KB, Berezovsky IN, Shakhnovich EI. 2007. Protein and DNA sequence determinants of thermophilic adaptation. *PLoS Comput Biol*. 3(1):e5.
- 89 Hensel F, Moor M, Rieck B. 2021. A survey of topological machine learning methods. *Front Artif Intell*. 4:681108.
- 90 Barnes D, Polanco L, Perea JA. 2021. A comparative study of machine learning methods for persistence diagrams. *Front Artif Intell*. 4:681174.
- 91 Qiu Y, Wei GW. 2023. Artificial intelligence-aided protein engineering: from topological data analysis to deep protein language models. *Brief Bioinform*. 24(5):bbad289.
- 92 Li W, et al. 2021. Refseq: expanding the prokaryotic genome annotation pipeline reach with protein family model curation. *Nucleic Acids Res*. 49(D1):D1020–D1028.
- 93 Burley SK, et al. 2023. RCSB protein data bank (RCSB.org): delivery of experimentally-determined PDB structures alongside one million computed structure models of proteins from artificial intelligence/machine learning. *Nucleic Acids Res*. 51(D1):D488–D508.
- 94 Altschul SF, et al. 1997. Gapped BLAST and PSI-BLAST: a new generation of protein database search programs. *Nucleic Acids Res*. 25(17):3389–3402.
- 95 Maria C, Boissonnat JD, Glisse M, & Yvinec M (2014) The gudhi library: simplicial complexes and persistent homology. In: Hong H, Yap C, editors. ICMS 2014. Berlin, Heidelberg: Springer Berlin Heidelberg. P. 167–174.
- 96 Katoh K, Standley DM. 2013. MAFFT multiple sequence alignment software version 7: improvements in performance and usability. *Mol Biol Evol*. 30(4):772–780.
- 97 Criscuolo A, Gribaldo S. 2010. BMGE (Block Mapping and Gathering with Entropy): a new software for selection of phylogenetic informative regions from multiple sequence alignments. *BMC Evol Biol*. 10:210.
- 98 Nguyen LT, Schmidt HA, von Haeseler A, Minh BQ. 2015. IQ-TREE: a fast and effective stochastic algorithm for estimating maximum-likelihood phylogenies. *Mol Biol Evol*. 32(1):268–274.
- 99 Kalyaanamoorthy S, Minh BQ, Wong TKF, von Haeseler A, Jermini LS. 2017. ModelFinder: fast model selection for accurate phylogenetic estimates. *Nat Methods*. 14(6):587–589.
- 100 Gouy M. 1987. Codon contexts in enterobacterial and coliphage genes. *Mol Biol Evol*. 4(4):426–444.
- 101 Bou Dagher L, Madern D, Malbos P, & Brochier-Armanet C (2024) Data for “Persistent homology reveals strong phylogenetic signal in three-dimensional protein structures”. *Mendeley Data*. <https://doi.org/10.17632/mhpcr6c827.1>